Efficiency of a torsional flutter harvester in thunderstorm-like turbulent winds: some recent results

Luca Caracoglia[1]

[1]*Northeastern University, Boston, MA 02115 USA, lucac@coe.neu.edu*

SUMMARY:
This study examines the efficiency of a torsional-flutter energy harvester in non-synoptic wind environments. The apparatus has been proposed as an alternative to other flapping mills of medium size. The study is inspired by works by Professor Solari that simulate the dynamic response of structures due to non-stationary, turbulent thunderstorm outflows. A sudden change of wind load intensity, typical of a thunderstorm downburst, may either impact energy conversion or ultimately damage the apparatus. A stochastic model is used to enable the investigation of both pre-critical and post-critical regimes. The study also explores aeroelastic load variability through suitable random perturbation to unsteady Wagner's indicial theory, which is combined with non-stationary turbulence effects. Various geometries are considered. They include variable width of the blade-airfoil, aspect ratio (transverse length to chord) of the apparatus, etc. The study shows that unsteady turbulence effects can have a beneficial effect on the performance by promoting instability.

Keywords: aeroelastic harvester, stochastic stability, thunderstorm winds

1. INTRODUCTION

Wind energy technology is rapidly evolving because of the need for green energy sources. While large wind turbines are employed to maximize output power, "specialized" harvesters have been proposed to exploit wind energy at low wind speeds. These harvesters are designed for medium scale applications, triggered by various aeroelastic instability phenomena (Abdelkefi et al., 2012; Bernitsas et al., 2008; Gkoumas et al., 2017; Matsumoto et al., 2006; Pigolotti et al., 2017; Shimizu et al., 2008). Along this line of research, a torsional-flutter-based apparatus has been proposed by Caracoglia (2018). Previous studies have examined the post-critical stability of the harvester and the operational conditions of the apparatus, under steady turbulent wind flows. However, the apparatus is designed to be used in any wind conditions and various installation configurations, e.g., non-ideal and non-stationary gust fronts. Therefore, the objectives of this study are to:

- utilize and adapt the current theory for the analysis of wind loads and structural response in non-synoptic, non-stationary thunderstorms (Solari, 2016) to wind energy;

- examine post-critical performance of the apparatus and its ability to be triggered by an imperfect wind flow and a thunderstorm-like turbulent gust front;

- derive a new and enhanced model, based on stochastic differential equations, and examine the mean-square stability limits of the apparatus.

2. DESCRIPTION OF THE APPARATUS AND CURRENT STATE OF THE RESEARCH

Figure 1 presents the schematics of the proposed apparatus, composed of a flapping blade-airfoil with pivot axis position designated with the symbol "O". The main dimensions of the harvester are half-chord length b, transverse length ℓ between adjacent, equidistant rotational (torsional) supports. A nonlinear torsional spring mechanism is designed to be installed at the equidistant supports (distance ℓ) to enable flapping of the blade-airfoil and torsional flutter.
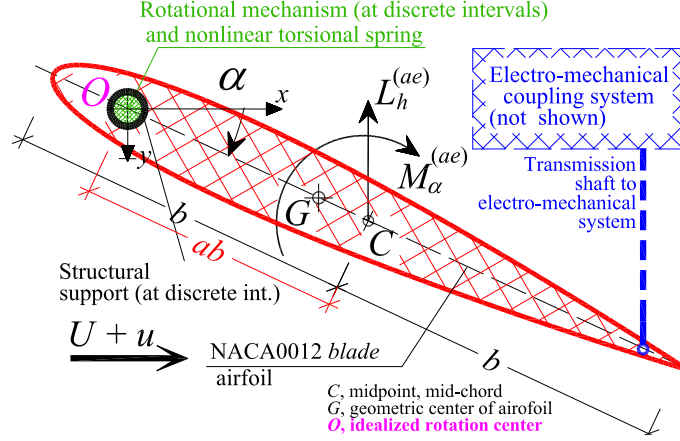

Figure 1. Schematics of the torsional flutter harvester - cross sectional view on XY horizontal plane.

Various configurations have been considered with adjustable position of the pivot rotation axis, *ab* in Fig. 1: pivot axis can be moved from the leading edge ($a = -1$) to the quarter-chord leeward position ($a \approx -0.75$). Furthermore, the half-chord width of the blade-airfoil b can vary between 0.25 and 1.00 m while the aspect ratio, defined as AR $= \ell/b$ (transverse length to chord) varies between four and ten. Lift force and torque reduction is considered due to three-dimensional flow around the airfoil and AR. The incoming wind flow is represented by the superposition of a mean wind speed U and along-wind turbulence u (Fig. 1). Other turbulence components are secondary given the orientation of the apparatus. The conversion to electrical power is possible through an eddy current converter with multi-coil magnetic field. The model has been thoroughly applied to examine propensity to post-critical vibration and conversion from kinetic to electric energy.

3. ENHANCED, NON-STATIONARY LOAD AND STOCHASTIC DYNAMIC MODEL

The dynamic flapping equilibrium equation (with rotation α, dimensionless time $\tau = t\omega_\alpha$) is:

$$\frac{\mathrm{d}^2\alpha}{\mathrm{d}\tau^2} + 2\zeta_\alpha\frac{\mathrm{d}\alpha}{\mathrm{d}\tau} + \alpha + \kappa\alpha^3 = \frac{M_{0z} + M_{(\mathrm{e.m.})}}{\omega_\alpha^2 I_{0\alpha}} \tag{1}$$

In Eq. (1), structural damping is simulated through linear term ζ_α; nonlinear restoring force effect is simulated by the term $\kappa\alpha^3$ with κ suitable constant; $I_{0\alpha}$ is the total polar mass moment of inertia about O; ω_α is the angular frequency of the linearized dynamic equation.

The torsional moment about O in Fig. 1 combines aeroelastic torque M_{0z} and electro-motive torque $M_{(\mathrm{e.m.})} = -(1-a)b\Phi_{(\mathrm{e.m.c.})}I(\tau)$, with $I(\tau)$ output current of the power system and $\Phi_{(\mathrm{e.m.c.})}$ the electro-mechanical coupling coefficient that couples magnetic induction with translation of a moving shaft. Mean aerodynamic forces and torque are zero if $\alpha \approx 0$. With uniform, smooth and

stationary flow, the dynamic aeroelastic torque depends on U only; the torque is modeled by standard flow memory theory, i.e., *Wagner*'s indicial function formulation (Bisplinghoff et al., 1955). The indicial function of the load is $\Phi(s) = \left[1 - c_1 e^{-d_1 s} - c_2 e^{-d_2 s}\right]$ with time $s = \tau U / (\omega_\alpha b)$ and (c_1, d_1, c_2, d_2) deterministic parameters (Jones, 1939).

First, aeroelastic load variability is considered through perturbation to $\Phi(s)$: the deterministic quantity d_2 becomes random by rewriting it as time dependent, $d_2 = d_{2,\mathrm{m}} + \delta_2(\tau)$, where $d_{2,\mathrm{m}}$ is the mean value and δ_2 is a zero-mean, Gaussian noise of standard deviation σ_{d2} that accounts for load measurement errors, load interference with the supports, etc.

Second, slowly-varying temporal intensification and decay of U during a thunderstorm is not considered since the apparatus is designed to be activated with minimum delay (e.g., few minutes), shorter than the typical thunderstorm duration. By contrast, turbulence u is simulated by a Gaussian process that influences the instantaneous speed, i.e., the dynamic pressure term is proportional to $[U + u(\tau)]^2 \approx U^2 + 2U u(\tau)$ [m/s^2]. Stationary turbulence is written in dimensionless form as $\hat{u}(\tau) = u(\tau)/U$ and is represented by reduced turbulence spectrum (Solari, 2016); the standard deviation $\sigma_{\hat{u}}$ is the turbulence intensity of the stationary process. Non-stationary thunderstorm-like turbulence is obtained by uniform modulation function φ_{mf} (Solari, 2016), applied as $u \times \varphi_{\mathrm{mf}}$, which simulates the passage of a thunderstorm gust front. Since the the projected area (ℓb) is small compared to turbulence length scales, the gust load is fully correlated.

The Itô-type differential equation of the stochastic model is derived from Eq. (1); the dynamic states of vector $\mathbf{W}_{\mathrm{em}}$ are torsional rotation α, α' or the derivative with respect to τ, aeroelastic states, dimensionless current of the power circuit (ι) and dimensionless turbulence variable $\hat{u}$:

$$\mathrm{d}\mathbf{W}_{\mathrm{em}} = \mathbf{q}_{\mathrm{em,NL}}\left(\mathbf{W}_{\mathrm{em}}; \varphi_{\mathrm{mf}}(\tau)\right)\mathrm{d}\tau + \sqrt{2\pi}\left[\mathbf{T}_{\mathrm{NL},\hat{u}}\left(\mathbf{W}_{\mathrm{em}}; \phi(\tau)\right)\mathrm{d}B_{\hat{u}}(\tau) + \mathbf{Q}_{\mathrm{L},\Delta 2}\mathbf{W}_{\mathrm{em}}\mathrm{d}B_{\Delta 2}(\tau)\right] \quad (2)$$

In Eq. (2) $\mathbf{q}_{\mathrm{em,NL}}$ is a nonlinear, drift vector; $\mathbf{Q}_{\mathrm{L},\Delta 2}$ is a linear diffusion matrix that controls the load perturbation δ_2; $\mathbf{T}_{\mathrm{NL},\hat{u}}$ is a nonlinear turbulence diffusion vector. The scalar, Wiener noise $B_{\Delta 2}(\tau)$ separately addresses load perturbations from $B_{\hat{u}}(\tau)$, used for turbulence perturbations. Dependency of $\mathbf{T}_{\mathrm{NL},\hat{u}}$ on both the variance of $\hat{u}$ on $\varphi_{\mathrm{mf}}(\tau)$ is noted in Eq. (2).

4. STOCHASTIC STABILITY

Asymptotic stability is analyzed through Moment Lyapunov Exponent (MLE) theory (Xie, 2005) because Eq. (2) is nonlinear. The MLE measures the propensity of the system's slow dynamics to exhibit diverging oscillations; the MLE is a generalized measure of damping. Since the MLE cannot usually be found in closed form (Xie, 2005), stability must be studied numerically. This entails that Eq. (2) is first solved in weak form, i.e., by numerical integration that is repeated several times through Monte-Carlo sampling (Xie, 2005). Second, stability is found through the study of:

$$\Lambda_{\mathbf{W}}(2) \approx \log_{\mathrm{e}}\left(\mathbb{E}\left[\|\mathbf{W}(\tau_l)\|^2\right]\right) / \tau_l \quad (3)$$

Eq. (3) numerically evaluates the MLE, where $\mathbb{E}[.]$ is the expectation operator applied to the Euclidean norm of the vector $\mathbf{W} = [\alpha, \alpha']^T$; Eq. (3) approximates the limit as $\tau_l \to +\infty$, i.e., $\Lambda_{\mathbf{W}}(2)$ is evaluated at a sufficiently large time $\tau_l > 0$. Eq. (3) is adequate to study mean-square stability for wind contaminated by non-stationary gust fronts, noting that the approximate, asymptotic value in Eq. (3) should be referred to a finite time τ_l greater than the thunderstorm duration.

5. NUMERICAL RESULTS: *FROZEN DOWNBURST* WIND STATE

Figure 2 shows an example of 2*nd* MLE stability results, derived using the hypothesis of wind field with *frozen downburst* turbulence (constant $\varphi_{\mathtt{mf}} = 1$) and reduced turbulence intensity $\sigma_{\hat{u}} = 2\%$. The random load effect δ_2 is neglected. The figure panels show the temporal variation of $\Lambda_{\mathbf{W}}(2)$ as time tends to $\tau_l = 250$. Various apparatuses are studied with front rotation axis ($a = -1$) and variable physical properties, i.e., Types 0, 1 and 2 (Caracoglia, 2018). All the apparatuses have the same AR $= 4$. The structural damping ratio is set to $\zeta_\alpha = 0.25\%$ for all cases while the angular frequency ω_α varies. Initial triggering conditions at $\tau = 0$ are set to a zero-mean, random flapping amplitude with standard deviation $2°$. In Fig. 2, Type-2 apparatus is unstable at $U = 14.2$ m/s, noting that $\Lambda_{\mathbf{W}}(2) > 0$ exhibits an asymptotically diverging trend at $\tau > 200$. By contrast, other apparatuses are not prone to instability in this U range.
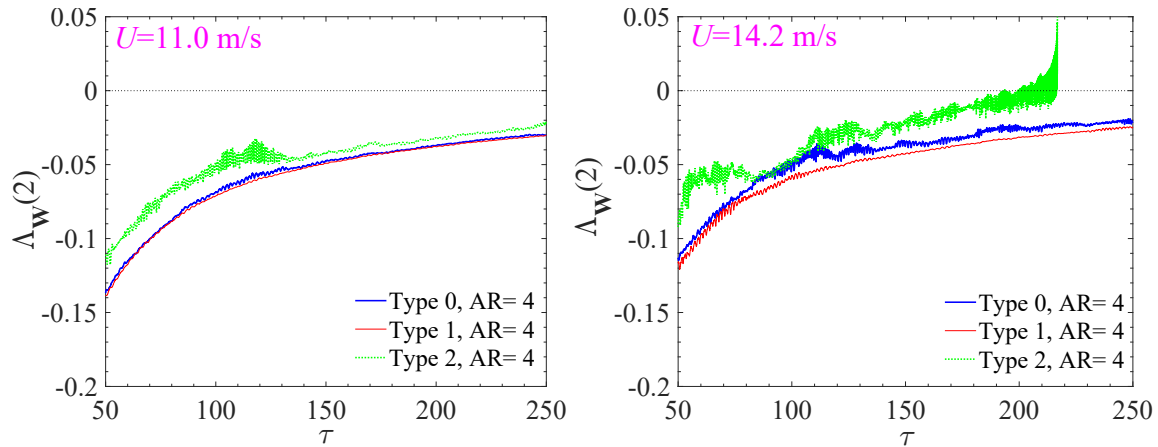

Figure 2. Stability of apparatus with front rotation axis ($a = -1$) in a frozen downburst turbulent wind state.

Deterministic post-critical analysis for Type-2 apparatus [$\omega_\alpha/(2\pi) = 0.10$ Hz and $b = 0.50$ m] without turbulence perturbations suggests that the device becomes active and produces energy at about $U = 15$ m/s. Consequently, downburst turbulence tends to reduce flutter speed, and has a positive influence on the operational conditions of the apparatus.

6. CONCLUSION AND OUTLOOK

More evidence is needed to confirm the preliminary remarks. Additional examples with variable configurations will be presented to study the combined effects of turbulence and load perturbations, as well as to demonstrate instability through Eq. (3) for a finite-duration thunderstorm. Alternate stability criteria and analysis methods may be explored.

REFERENCES
Abdelkefi, A., Nayfeh, A. H., and Hajj, M. R., 2012. Design of piezoaeroelastic energy harvesters. Nonlinear Dynamics 68, 519–530.

Bernitsas, M. M., Raghavan, K., Ben-Simon, Y., and Garcia, E. M. H., 2008. VIVACE (Vortex Induced Vibration Aquatic Clean Energy): A new concept in generation of clean and renewable energy from fluid flow. Journal of Offshore Mechanics and Arctic Engineering 130, 041101.

Bisplinghoff, R., Ashley, H., and Halfman, R., 1955. Aeroelasticity. Dover Publications Inc., Mineola, NY, USA.

Caracoglia, L., 2018. Modeling the coupled electro-mechanical response of a torsional-flutter-based wind harvester with a focus on energy efficiency examination. J. Wind Eng. Ind. Aerodyn. 174, 437–450.

Gkoumas, K., Petrini, F., and Bontempi, F., 2017. Piezoelectric vibration energy harvesting from airflow in HVAC (Heating Ventilation and Air Conditioning) systems. Procedia Engineering 199, 3444–3449.

Jones, R. T., 1939. *The unsteady lift of a finite wing*. Technical Note 682. NACA.

Matsumoto, M., Okubo, K., and Keisuke M. Ito, Y., 2006. Fundamental study on the efficiency of power generation system by use of the flutter instability. Proceedings of Proceedings 2006 ASME Pressure Vessels and Piping Division Conference. American Society of Mechanical Engineers, ASME Paper No. PVP2006–ICPVT11–93773.

Pigolotti, L., Mannini, C., Bartoli, G., and Thiele, K., 2017. Critical and post-critical behaviour of two-degree-of-freedom flutter-based generators. J. Sound Vibr. 404, 116–140.

Shimizu, E., Isogai, K., and Obayashi, S., 2008. Multiobjective design study of a flapping wind power generator. J. Fluids Eng.-ASME 130, 021104.

Solari, G., 2016. Thunderstorm response spectrum technique: Theory and applications. Eng. Struct. 108, 28–46.

Xie, W.-C., 2005. Monte carlo simulation of moment Lyapunov exponents. J. Appl. Mech. 72, 269–275.